International Journal of Science and Research (IJSR)
ISSN (Online): 2319-7064
Index Copernicus Value (2013): 6.14 | Impact Factor (2015): 6.391

Optimum Channel Combinations for Retrieval of Oceanic Winds Using a Radiometer

Thomas Mathew

Gujarat National Law University, Gandhinagar-382007, India
Email: thomas_mathew_tm[at]yahoo.com

Abstract: ***The most part of the earth is covered with water and so it becomes imperative to have a better knowledge about the oceanic winds so as to know/predict the climatic changes. There are several sensors but radiometer being a passive microwave sensor has its own advantages in the study of oceanic winds. The radiometer generally operates at various frequencies and the capacity to retrieve information increases with the usage of V and H polarizations of the frequency. This paper is an attempt to understand and check for the optimum channel combination(s) from amongst the frequencies being used by the radiometer, for the retrieval of oceanic winds.***

Keywords: radiometer, emissivity, wind

1. Introduction

Radiometers are passive microwave systems [1], which measure microwave emissions from objects, generated due to collisions of molecules inside the object, at various frequencies and polarizations. Spaceborne microwave radiometers on polar satellites with a fairly high repetitive frequency are being used for sensing the earth's surface and the atmosphere globally. A large number of microwave radiometers have been flown on satellites as on date for various applications related to land, ocean and atmosphere.

Radiometry is the measurement of incoherent radiant electromagnetic energy. Passive microwave radiometry measures naturally emitted microwave energy (also expressed as brightness temperature), which is based on a surface's physical, electrical and thermodynamic variables. The ocean surface's properties affect physical-electrical interactions, which then determine the surface's microwave emission [2].

Microwave radiometry is mainly used because it is independent of the sun and can penetrate clouds, rain and other objects to an extent. Microwaves have a penetration larger than that obtainable with visible and infrared radiation into the ground, or ocean surface. The observation in the microwave region is a result of geometric and bulk-dielectric properties, whereas in the infrared and visible region it is the result of molecular resonances in the surface layer. Spaceborne radiometers typically have many measurement channels like the AMSR-E has 12 channels viz., six frequencies each with H- and V-polarization data streams. However, the high correlation between data channels does not allow twelve different parameters to be extracted from the data set.

2. Geophysical Parameter Retrieval

There are three broad types of approach to the development of geophysical parameter (Sea Surface Temperature, Surface Wind Speed, Cloud Liquid Water, Total Water Vapour, Rain Rate) retrieval algorithm: multiple linear regression, non-linear iterative, and post-launch in-situ regression. The first two approaches are geophysical algorithms as they rely on physically based Radiative Transfer Models (RTMs) of the ocean and atmosphere. The third is purely statistical, based on regression between satellite and in situ observations. While this approach may have the smallest root mean square deviation (RMSD) when compared to in-situ data, understanding the underlying physical basis for the algorithm (leading to improvements) is not possible. The microwave radiation at frequencies < 15 GHz is insensitive to atmospheric aerosols and is only weakly attenuated by oxygen, non-precipitating clouds, and atmospheric water vapour. However, it is strongly attenuated and scattered by precipitation. The radiative transfer equation has to be regressed against multiple parameters in order to retrieve the geophysical parameter such as sea surface temperature, wind speed, water vapour, cloud liquid water, rain rate etc. Attenuation accounts for ~ 3% of the signal received, but simultaneous retrieval using additional frequencies (19-85 GHz) allows for an extremely accurate correction.

3. Sea Surface Wind Speed

The microwave emission from the ocean depends on surface roughness [3]. A calm sea surface is characterized by a highly polarized emission. When the surface becomes rough, the emission increases and becomes less polarized (except at incidence angles above 55° for which the vertically polarized emission decreases). There are three mechanisms that are responsible for this variation in the emissivity. First, surface waves with wavelengths that are long compared to the radiation wavelength depolarize the initial horizontal and vertical polarization states and change the local incidence angle. This phenomenon can be modeled as a collection of tilted facets, each acting as an independent specular surface [4]. The second mechanism is sea foam and the Sea foam models have been developed [5], [6]. The third roughness effect is the diffraction of microwaves by surface waves that are small compared to the radiation wavelength. These three effects can be parameterized in terms of the rms slope of the large-scale roughness, the fractional foam coverage, and the rms height of the small-scale waves. Each of these parameters depends on wind speed. Cox and Munk; Monahan and O'Muircheartaigh; and Mitsuyasu and Honda derived wind speed relationships for the three parameters, respectively [7] - [9]. These wind speed relationships in conjunction with the tilt, foam and diffraction model provide the means to

compute the sea-surface emissivity. Computations of this type have been done by Wentz [10], [11] and are in general agreement with microwave observations.

4. Microwave Radiative Transfer Model

A parallel monochromatic beam of electromagnetic radiation propagates in vacuum without any change in its intensity however, if a small particle, is interposed into the beam, it can cause effects like absorption, emission, scattering and extinction. When electromagnetic radiation propagates through a medium and undergoes changes because of absorption, emission and scattering, the medium is referred to as a radiatively participating medium. The governing equation for radiative transfer in participating medium involves the three effects (absorption, emission and scattering) and turns out to be an integro-differential equation in term of intensity. The retrieval scheme that links the brightness temperature to physical parameters (rain rate, cloud liquid water, cloud ice, precipitating ice) is regularly set up as an optimization problem that utilizes forward model simulations [12]. Numerical models are used to compute the microwave radiation within a well-defined atmosphere. Accurate and computationally efficient forward radiative transfer calculations are essential for the retrieval of atmospheric and oceanic constituents from remotely sensed microwave satellite observations [13].

The development of forward model includes three steps. The first step is to generate the physical atmosphere, the second step is to convert the physical parameters into the radiative interaction parameters and the third step is to calculate the radiances leaving top of the atmosphere by solving the radiative transfer equations using the calculated interaction parameters. The radiative transfer model gives the simulated brightness temperatures for each viewing angle and frequency, for a downward looking space borne radiometer. The plane parallel solution is sufficient to cover most applications for radiation scattering in planetary atmospheres. The radiative interaction parameters (surface reflectivities, extinction, scattering albedo and phase matrix) are given as input for the radiative transfer calculations. The schematic diagram of the microwave radiative transfer model is shown in figure 1.

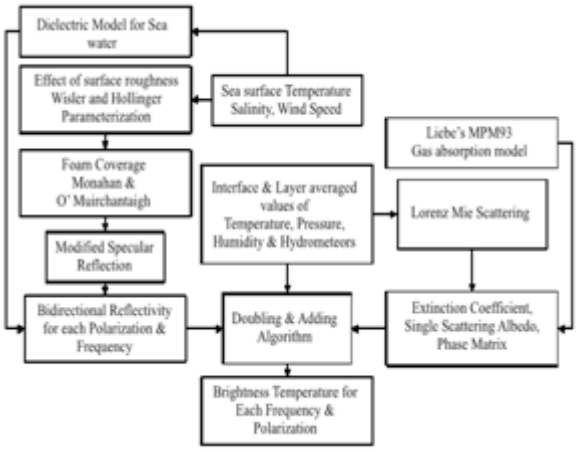

Figure 1: Schematic diagram of the microwave radiative transfer model (Adapted from [14]).

Following the doubling-adding algorithm described by Evans and Stephens to compute polarized radiation in plane parallel atmosphere, the monochromatic plane parallel polarized radiative transfer equation for randomly oriented particles is written as [14],

$$\mu \frac{dI}{d\tau}(\tau',\mu,\phi) = -I(\tau',\mu,\phi) + \frac{\tilde{\omega}}{4\pi}\int_0^{2\pi}\int_{-1}^{1} P(\mu,\phi;\tilde{\mu},\tilde{\phi})\, d\tilde{\mu}\, d\tilde{\phi} + (1-\tilde{\omega})B(T)\begin{bmatrix}1\\0\\0\\0\end{bmatrix}$$

Here I is the diffuse radiance field expressed as the vector of four Stokes parameters (I,Q,U,V), P is the 4×4 scattering (or Mueller) matrix, B(T) is the Planck blackbody function, $\tilde{\omega}$ the single scattering albedo, τ' the optical depth, μ the cosine of the zenith angle θ and ϕ the azimuth angle. The angular variation of radiation is written as a Fourier series in the azimuth direction and by discretization in the zenith angle using numerical Gaussian quadrature. The radiance at any position inside the atmosphere is represented by Stokes parameters, quadrature zenith angles and the Fourier azimuth modes.

5. Methodology to determine the optimum channel combinations for retrieval of oceanic winds

The brightness temperatures and wind speed were generated for noise-free condition using the Forward Radiative Transfer Model mentioned in section 4. The brightness temperatures and wind speeds were generated for the vertical and horizontal polarizations of various frequency channels viz., 6.9, 10.65, 18.7, 23.8 and 36.5, predominantly used in the various radiometric missions carried out till today across the world by various organizations. Seventy percent of the generated points were used to generate the algorithm for various channel combination using the regression analysis. The remaining thirty percent points were used to validate the generated equation for which the correlation coefficient and rmsd was found. From amongst the possible combinations, the combinations with the least rmsd have been depicted in table 1 and the variation of the rmsd with respect to the number of channel combinations has been shown in figure 2.

The actual brightness temperatures obtained from the radiometer will be affected by the interaction of the electromagnetic wave with various types of constituents in its path of propagation and these altercations in the brightness temperatures are known as noises. In order to introduce the noise into the generated brightness temperatures mentioned above, Box-Muller Transformation was used to generate the Gaussian distribution for each brightness temperature. Again, seventy percent of these generated points were used to generate the algorithm for various channel combination using the regression analysis. The remaining thirty percent points were used to validate the generated equation for which the correlation coefficient and rmsd were found. From amongst the possible combinations, the combinations with the least rmsd have been depicted in table 2 and the variation of the rmsd with respect to the number of channel combinations has been shown in figure 3.

6. Conclusion

The study depicts uniformity in nine channel combinations in both the cases viz., without and with noise, as both showed that the best combination is for without 6.9H channel being used. However, the coefficients did differ in both the cases.

In case of 3 to 8 channel combinations for both without and with noise, it has been found that 6.9V and 10.65 channels play a dominant role, with other channels showing their significance but with no uniformity.

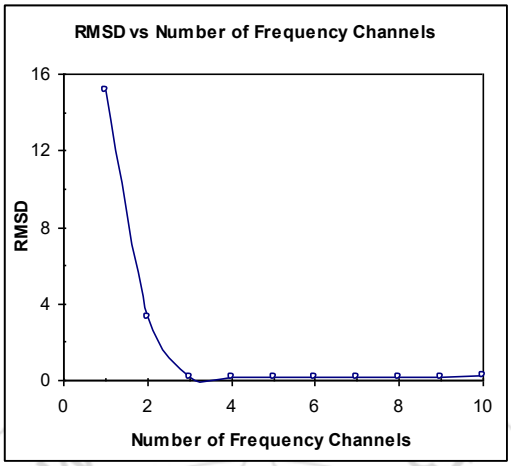

Figure 2: Variation of RMSD with respect to the number of frequency channels for the brightness temperatures without noise effect.

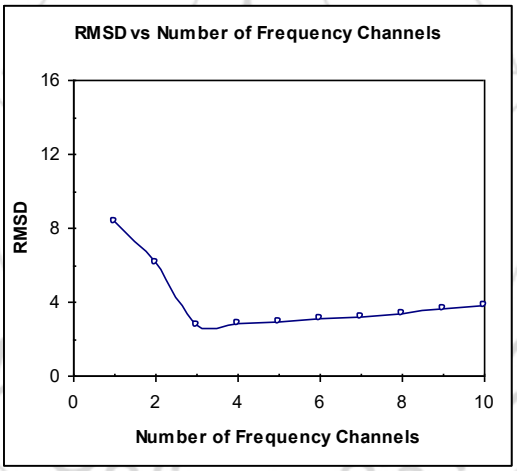

Figure 3: Variation of RMSD with respect to the number of frequency channels for the brightness temperatures with noise effect.

Table 1: Details of the channel combinations with least rmsd for the brightness temperatures without noise effect

No. of Channels	*Channel Combination*	*Corr. Coeff*	*RMSD*
1	10.65V	0.991	15.17
2	6.9V, 10.65V	0.9918	3.29
3	6.9V, 10.65V, 36.5V	0.9991	0.15
4	6.9V, 10.65V, 23.8V, 36.5V	0.9991	0.13
5	6.9V, 10.65V, 18.7V, 23.8V, 36.5V	0.9991	0.13
6	6.9V, 10.65V, 10.65H, 18.7V, 23.8H, 36.5H	0.9999	0.19
7	6.9V, 10.65V, 10.65H, 18.7V, 18.7H, 23.8V, 36.5H	0.9999	0.21
8	6.9V, 10.65V, 10.65H, 18.7V, 18.7H, 23.8V, 36.5V, 36.5H	0.9999	0.17
9	6.9V, 10.65V, 10.65H, 18.7V, 18.7H, 23.8V, 23.8H, 36.5V, 36.5H	0.9999	0.17
10	6.9V, 6.9H, 10.65V, 10.65H, 18.7V, 18.7H, 23.8V, 23.8H, 36.5V, 36.5H	0.9999	0.22

Table 2: Details of the channel combinations with least rmsd for the brightness temperatures with noise effect

No. of Channels	*Channel Combination*	*Corr. Coeff*	*RMSD*
1	10.65V	0.6604	8.37
2	6.9V, 10.65V	0.7616	6.12
3	6.9V, 10.65V, 23.8H	0.9045	2.73
4	6.9V, 10.65V, 23.8V, 36.5H	0.9547	2.83
5	6.9V, 10.65V, 18.7V, 23.8V, 36.5H	0.9555	2.96
6	6.9V, 10.65V, 23.8V, 23.8H, 36.5V, 36.5H	0.9648	3.07
7	6.9V, 10.65V, 18.7V, 23.8V, 23.8H, 36.5V, 36.5H	0.965	3.16
8	6.9V, 10.65V, 18.7V, 18.7H, 23.8V, 23.8H, 36.5V, 36.5H	0.9765	3.36
9	6.9V, 10.65V, 10.65H, 18.7V, 18.7H, 23.8V, 23.8H, 36.5V, 36.5H	0.9816	3.64
10	6.9V, 6.9H, 10.65V, 10.65H, 18.7V, 18.7H, 23.8V, 23.8H, 36.5V, 36.5H	0.9834	3.84

In the noise-free noise, it has been found that for the brightness temperature of the 36.5V channel plays a crucial role for the three, four and five channel combinations. On the contrary, in with-noise case for three channel combinations it is the 23.8H and for four and five channel combinations it is the 36.5H channel which plays a significant role. In six, seven and eight channel combinations for noise-free and with-noise, all channels remain the same except for 10.65H which plays a significant role in the noise-free case. In case of with-noise, 36.5V for 23.8H play a significant role in six and seven; and seven and eight channel combinations respectively.

This study on the whole leads one to infer that a set of four or five channels (consisting of 6.9V, 10.65V, 18.7V, 23.8V, 36.5H) are adequate for sensing surface wind speed with reasonable accuracy. The 6.9 GHz and 10.65 GHz channels play a significant role as they are surface channels (i.e. they are more sensitive to surface parameters and less sensitive to atmospheric parameters). The atmospheric channels (like 23 GHz) are used for correcting the atmospheric effects. But primary channels for surface winds are 6.9 GHz and 10.65 GHz. Adding more channels does not necessarily increase the accuracy of the retrieved parameter.

Acknowledgement

The author is thankful to Dr. Abhijit Sarkar, the Ph.D. Guide for constant guidance and to all the members of Space Applications Centre, Ahmedabad for their constant support especially Mr. Abhishek Chakraborty.

References

[1] F. T. Ulaby, R. K. Moore and A. K. Fung, Microwave Remote Sensing: Active and Passive, Vol. I, Artech House, Inc., Norwood, MA, 1981.
[2] I. S. Robinson, Measuring the Oceans from Space: The principles and methods of satellite oceanography, Praxis Publishing Ltd., Chichester, UK, 2004.
[3] F. J. Wentz, "Measurement of oceanic wind vector using satellite microwave radiometers", IEEE Transactions on Geoscience and Remote Sensing, 30 (5), pp. 960 – 972, 1992.
[4] L. Ferranti, J. M. Slingo, T. N. Palmer and B. J. Hoskins, "Relations between interannual and intraseasonal monsoon variability as diagnosed from AMIP integrations", Quarterly Journal of the Royal Meteorological Society, 123 (541), pp. 1323 – 1357, 1997.
[5] A. Stogryn, "The Emissivity of Sea Foam at Microwave Frequencies", Journal of Geophysical Research, 77 (9), pp. 1658 – 1666, 1972.
[6] P. M. Smith, "The emissivity of sea foam at 19 and 37 GHz", IEEE Transactions on Geoscience and Remote Sensing, 26 (5), pp. 541 – 547, 1988.
[7] C. Cox and W. Munk, "Measurement of the Roughness of the Sea Surface from Photographs of the Sun's Glitter", Journal of the Optical Society of America, 44 (11), pp. 838 – 850, 1954.
[8] E. C. Monahan and I. Ó. Muircheartaigh, "Optimal Power – Law Description of Oceanic Whitecap Coverage Dependence on Wind Speed", Journal of Physical Oceanography, 10 (12), pp. 2094 – 2099, 1980.
[9] H. Mitsuyasu and T. Honda, "Wind – induced growth of water waves", Journal of Fluid Mechanics, 123, pp. 425 – 442, 1982.
[10] F. J. Wentz, "A Two – Scale Scattering Model for Foam – Free Sea Microwave Brightness Temperatures", Journal of Geophysical Research, 80 (24), pp. 3441 – 3446, 1975.
[11] F. J. Wentz, "A Model Function For Ocean Microwave Brightness Temperatures", Journal of Geophysical Research, 88 (C3), pp. 1892 – 1908, 1983.
[12] S. P. Venkateshan, C. Balaji, M. Deiveegan, V. K. Agarwal and R. M. Gairola, "Development of a Generalized Radiative Transfer Model Including Polarization and Robust Retrieval Algorithms to Obtain Geophysical Parameters Over Sea and Land Surfaces Using Microwave Remote Sensing Data", Project No: ICSR/ISRO – IIT (M) /MEE/086/04 – 05/SPVE, Indian Institute of Technology Madras, India, 2007.
[13] G. W. Petty, "Physical and Microwave Radiative Properties of Precipitating Clouds. Part I: Principal Component Analysis of Observed Multichannel Microwave Radiances in Tropical Stratiform Rainfall", Journal of Applied Meteorology, 40 (12), pp. 2105 – 2114, 2001.
[14] C. Balaji, M. Deiveegan, S. P. Venkateshan, R. M. Gairola, A. Sarkar and V. K. Agarwal, "Polarized microwave forward model simulations for tropical storm Fanoos", Journal of Earth System Science, 118 (4), pp. 331 – 343, 2009.